2011-05

The 2nd Generation of Safety Fans GUI

Mulloy, C.C.

Mulloy, C.C., Tiaden, R.D, and Yakimenko, O.A., “The 2nd Generation of Safety Fans GUI,” Proceedings of the 21st AIAA Aerodynamic Decelerator Systems Technology Conference, Dublin, Ireland, May 23-26, 2011.
http://hdl.handle.net/10945/50412

21st AIAA Aerodynamic Decelerator Systems Technology Conference and Seminar
23 - 26 May 2011, Dublin, Ireland

AIAA 2011-2603

The 2nd Generation of Safety Fans GUI

Craig C. Mulloy[1], Ryan D. Tiaden[2]
The U.S. Army Yuma Proving Ground, Yuma, AZ 85365

Oleg A. Yakimenko[3]
Naval Postgraduate School, Monterey, CA 93943

This paper deals with the continuing development of a multistage aerodynamic delivery systems safety tool currently being used in conjunction with aerodynamic deceleration payload delivery systems testing at the U.S. Army Yuma Proving Ground. This tool was created to assist test planning officers with safety related concerns involving air delivery tests and was introduced at the previous Aerodynamic Decelerator Systems (ADS) conference. Present paper presents the latest version of this tool incorporating multiple airdrops per pass, elevation data and more accurate models of the payload delivery systems accounting for their weight and the altitude of a drop zone.

Nomenclature

x, y, h	=	system's Northing, Easting and altitude
x_o, y_0	=	Northing and Easting at the altitude of canopy deployment
$w(h), \psi(h)$	=	speed and direction of the wind at altitude h
$v(h)$	=	descent rate at altitude h
GR	=	glide ratio
C_d	=	drag coefficient
ρ	=	air density
g	=	gravity
S	=	reference area
m	=	mass of the system
v_0	=	descent rate at sea level

I. Introduction

An ongoing revision process has increased the functionality of the Graphical User Interface (GUI) (ref 1) and revised the formulas and algorithms used to compute the gliding trajectory and safety danger zone (SDZ) for a multiple-stage aerodynamic deceleration system. Additions to the GUI include the ability to compute the release point based on the gliding trajectory and intended point of impact (IPI), the ability to release multiple delivery systems on a single pass, the ability to incorporate topography in the shape of the safety fan, and the ability to differentiate between pressure altitude and true altitude. This tool also includes a capability to convert any wind profile to a ballistic wind profile, used by some other programs as input data. These modifications have increased the accuracy of the computations, which is demonstrated in this paper on several examples.

The primary revision to the algorithms used in SDZ calculations include the addition of a variable rate of descent that is dependent upon altitude (air density). Current Air Force procedures (ref 2) used to calculate a Computed Air Release Point (CARP) are based on average parachute ballistics and assume a constant rate of descent from release to impact. These procedures are designed to minimize errors while providing ease of preflight and inflight mission planning in a live combat situation. Determining the average rate of descent from release to impact also adds further complexity to CARP calculations. The GUI under discussion in this paper will be used in a controlled test

[1] Test Officer / Aerospace Engineer, Air Delivery and Soldier Systems, U.S. Army Yuma Proving Ground, ATTN: TEDT-YPY-AAV, craig.mulloy@us.army.mil, Member AIAA.
[2] Team Leader / Aerospace Engineer, Air Delivery and Soldier Systems, U.S. Army Yuma Proving Ground, ATTN: TEDT-YPY-AAV, ryan.tiaden@us.army.mil, Member AIAA.
[3] Professor, Department of Systems Engineering, Code SE/Yk, oayakime@nps.edu, Associate Fellow AIAA.

environment with readily available access to more sophisticated computing technologies, and thus, more sophisticated algorithms may be used. The incorporation of a variable rate of descent will improve the accuracy of unguided airdrops by decreasing missed distance from the IPI.

This paper is organized as follows. Section II develops the mathematical foundation to incorporate a variable rate of descent and the ability to differentiate between pressure altitude and true altitude. Section III presents a comparison of a SDZ computed using the old algorithms (constant rate of descent) with the new algorithms (variable rate of descent), as well as the corresponding software to implement these algorithms. Section IV presents an in depth guide to using the GUI and the new features that have been incorporated since the original version that was presented at the previous ADS conference. Section V discusses the future of the GUI, including planned features and improvements. The paper ends with conclusions.

II. Computations

This section considers a single stage parachute system with a fully inflated canopy. The effect of winds will be calculated to determine the gliding path of the system; any ballistic period that would normally occur before full inflation is ignored in this analysis.

First, the formulas to incorporate a variable rate of descent for this single stage system will be developed. It will also be shown the error that can be expected should a constant rate of descent be used instead. Second, the formula to differentiate between pressure altitude and true altitude will be developed. This feature is especially helpful for airdrops occurring above 18,000 ft Mean Sea Level (MSL), the transition altitude in the United States.

A. Variable Rate of Descent

Currenlty, average rate of descent is determined by averaging the rate of descent at the release altitude with the rate of descent at sea level. Using the new algorithm described below, only sea level rate of descent is required as a GUI input. The program will automatically take air density and altitude into account. Using an average rate of descent poses three problems when calculating a gliding trajectory for a system. First, the change in descent rate with respect to altitude is not linear. This nonlinearity introduces an error when average descent rate is used. Second, the descent rate at the release altitude must still be calculated to determine the average descent rate. In other words, using the average descent rate is not any simpler or easier for the user than using sea level descent rate. Third, using an average descent rate gives equal weight to the winds throughout the flight. Winds at 20,000 ft MSL will not affect the system in the same way winds at 2,000 ft MSL would since the system is falling faster at the higher altitude.

The basic formula for the forces acting on an ADS in flight is

$$\frac{1}{2}C_d\rho v^2 S = mg \tag{1}$$

The basic formula for air density changing with altitude is

$$\rho = 1.225\left(1 - 0.0065\frac{\boldsymbol{h}[m]}{288.15}\right)^{4.2559}\left[\frac{kg}{m^3}\right] \tag{2}$$

Here, the formula corresponds to standard atmosphere and MSL altitude. There are two uncertain factors: $m = var$, and $\rho = \rho(\boldsymbol{h})$. Additionally, there is a third unpredictable factor: a non-standard atmosphere with the inverse temperature layer by the surface of the Earth. With the nominal mass m^*, the descent rate at sea level $(\boldsymbol{h} = 0)$ is v_0. According to Eq.(2) at a release altitude of 3 km MSL, $\rho_3 = 0.74\rho_0$. Rewriting Eq.(1) as

$$\rho v^2 = \frac{2mg}{C_d S} = const \tag{3}$$

results in

$$\rho_{\mathbf{0}} v_{\mathbf{0}}^{\mathbf{2}} = \rho v^{\mathbf{2}} \tag{4}$$

or

$$v = \sqrt{\frac{\rho_{\mathbf{0}}}{\rho}} v_{\mathbf{0}} \tag{5}$$

Hence, using standard atmosphere at an altitude of 7.5 km MSL, $p_{7.5} = 0.557 p_{\mathbf{0}}$ and $v_{7.5} = 1.48 v_{\mathbf{0}}$. It is seen here that the descent rate at 7.5 km MSL is almost 50% higher than the sea level descent rate. Let us do something else. Express Eq. (1) as

$$v = \sqrt{\frac{2mg}{C_d \rho S}} = \rho^{-0.5} const \tag{6}$$

Take a variation of Eq. (6)

$$\delta v = -0.5 \delta\rho\rho^{-1.5} const \tag{7}$$

Divide Eq. (7) by Eq. (6) to arrive at

$$\frac{\delta v}{v} = -0.5 \frac{\delta \rho}{\rho} \tag{8}$$

To summarize, a 1% decrease in air density leads to a 0.5% increase of the descent rate.

With these basic formulas and relationships, a set of equations[1] can be derived to calculate the gliding path of a system whose canopy has successfully deployed. Assuming that forward throw and aerodynamic drag can be neglected:

$$\frac{dx}{dt} = w(\boldsymbol{h}) \cos \psi_w(\boldsymbol{h}) + v(\boldsymbol{h}) GR cos\psi$$

$$\frac{dy}{dt} = w(\boldsymbol{h}) \sin \psi_w(\boldsymbol{h}) + v(\boldsymbol{h}) GR sin\psi \tag{9}$$

$$\frac{d\boldsymbol{h}}{dt} = v(\boldsymbol{h})$$

Here, horizontal motion is caused by wind and the system's glide ratio and vertical motion is caused by gravity. While the glide ratio remains constant throughout the flight, wind speed, wind direction, and rate of descent change with altitude (air density). Using the third equation to reduce the first two equations yields:

$$\frac{dx}{d\boldsymbol{h}} = \frac{w(\boldsymbol{h}) cos\psi(\boldsymbol{h})}{v(\boldsymbol{h})} + GR cos\psi$$

$$\frac{dy}{d\boldsymbol{h}} = \frac{w(\boldsymbol{h})sin\psi(\boldsymbol{h})}{v(\boldsymbol{h})} + GRsin\psi \tag{10}$$

Integrating these equations with respect to altitude results in:

$$x(\boldsymbol{h}) = x_{\boldsymbol{0}} + \int_{\boldsymbol{h}}^{H_{\boldsymbol{0}}} [(v]^{-1}(h)w(h)\mathbf{cos}\psi(\mathbf{h}) + GRcos\psi)d\boldsymbol{h}$$

$$y(\boldsymbol{h}) = y_{\boldsymbol{0}} + \int_{\boldsymbol{h}}^{H_{\boldsymbol{0}}} [(v]^{-1}(h)w(h)\mathbf{sin}\psi(\mathbf{h}) + GRsin\psi)d\boldsymbol{h} \tag{11}$$

Now, separating these equations into two parts, the wind component and the glide component:

$$x(\boldsymbol{h}) = x_{\boldsymbol{0}} + \int_{\boldsymbol{h}}^{H_{\boldsymbol{0}}} \frac{w(h)\cos\psi(\mathbf{h})}{v(h)}\mathbf{dh} + (H_0 - h)GRcos\psi$$

$$y(\boldsymbol{h}) = y_{\boldsymbol{0}} + \int_{\boldsymbol{h}}^{H_{\boldsymbol{0}}} \frac{w(h)\sin\psi(\mathbf{h})}{v(h)}\mathbf{dh} + (H_0 - h)GRsin\psi \tag{12}$$

If the variable winds, $w(\boldsymbol{h})$, and rate of descent, $v(\boldsymbol{h})$, are given in a look-up table as elements w_k and v_k, then the effect of winds from Eq. (12) can be reduced to the following:

$$\int_{\boldsymbol{h}}^{H_{\boldsymbol{0}}} \frac{w(\boldsymbol{h})cos\psi(\boldsymbol{h})}{v(\boldsymbol{h})}d\boldsymbol{h} \approx \sum_{k=m}^{M-\boldsymbol{1}} \frac{w_{k+\boldsymbol{1}}cos\psi_{k+\boldsymbol{1}}(\boldsymbol{h}_{k+\boldsymbol{1}} - \boldsymbol{h}_k)}{v_k}$$

$$\int_{\boldsymbol{h}}^{H_{\boldsymbol{0}}} \frac{w(\boldsymbol{h})sin\psi(\boldsymbol{h})}{v(\boldsymbol{h})}d\boldsymbol{h} \approx \sum_{k=m}^{M-\boldsymbol{1}} \frac{w_{k+\boldsymbol{1}}sin\psi_{k+\boldsymbol{1}}(\boldsymbol{h}_{k+\boldsymbol{1}} - \boldsymbol{h}_k)}{v_k} \tag{13}$$

where

$$v_k = \sqrt{\frac{\rho_{\boldsymbol{0}}}{\rho_k}}v_{\boldsymbol{0}} \tag{14}$$

Using Eq. (5), rate of descent is shown to be dependent on sea level rate of descent and air density. If no current source of meteorological data is available, then equation Eq. (2) may be used to approximate the change in density with altitude.

B. Pressure Altitude

When flying in the United States above an altitude of 18,000 ft MSL, aircraft use pressure altitude calibrated to the international standard pressure datum of 1013.25 hPa (29.92 in Hg). In areas where the atmosphere differs significantly from standard atmosphere, the true altitude can also significantly differ from pressure altitude. Here the calculations are presented to convert pressure altitude into true altitude using a true meteorological source.

First, let us assume the user has opted to input altitude as pressure altitude. First, this altitude must be converted into a pressure reading. Using the standard pressure datum of 1013.25 hPa, the pressure at a given altitude is

$$P[hPa] = 1013.25 * (1 - h[m] * 2.25577x10^{-5})^{5.25588} \tag{15}$$

If a true meteorological source has been selected, the true altitude can be found by interpolating and matching the calculated pressure from Eq.(15) to the corresponding true altitude with the same pressure. An example will now be presented to demonstrate this process. Let us assume an airdrop altitude of 7,000 m:

$$P = 1013.25 * (1 - 7000 * 2.25577x10^{-5})^{5.25588} = 410.6$$

YPG uses the RAWIN weather ballon as the primary source of current meteorological data. The following data from a YPG RAWIN weather balloon will now be used:

Altitude (M above msl)	Press (hPa)	Temp (°C)	RH (%)	Dew Pt Temp (°C)	Air Density (g/m^3)	Wind Direct (degs)	Wind Speed (m/s)
7000	434.1	-16.2	19	-34.4	587.75	298.6	9.1
7100	428.3	-16.6	11	-40.6	581.00	289.2	6.9
7200	422.6	-17.3	7	-45.5	574.92	272.7	6.1
7300	417.1	-18.0	4	-49.8	568.84	252.3	6.1
7400	411.4	-17.6	3	-53.7	560.37	229.4	5.7
7500	406.0	-17.6	2	-56.6	552.97	235.0	4.8
7600	400.6	-18.3	2	-56.7	547.12	238.4	4.9
7700	395.2	-18.8	2	-57.2	540.85	232.0	4.5
7800	390.0	-19.6	2	-56.8	535.33	217.9	3.6
7900	384.7	-20.5	2	-57.1	529.98	216.4	3.4

Interpolating for a pressure of 410.6 hPa yields a corresponding altitude of 7,412 m. This represents a difference of 412 m from the desired airdrop altitude. This difference can significantly affect both the gliding trajectory calculations and the size of the safety fan. For example, using the calculated difference of 412 m and a glide ratio of 3:1, the safety fan radius would be over 1,200 m larger. Furthermore, the effect of winds will be more significant as the system will have a longer flight time. Correcting for this altitude will yield a more accurate gliding trajectory and a more accurate safety fan, both of which will improve safety for those involved with testing.

III. Comparison of Safety Fans for a One-Stage System

Consider a system that has one stage and a sea level, standard atmosphere descent rate of 9 meters per second (m/s). A comparison will now be made using the original algorithm which assumed a constant rate of descent from release to impact, with the revised algorithm which corrects the rate of descent with altitude (air density). This comparison will be done using a standard atmosphere model, as well as actual meteorological data as recorded using a YPG RAWIN weather balloon.

Building off of the original GUI, the following fragments of Matlab code incorporate a variable rate of descent. Assume the system is released from an altitude of h = 7,000 m Above Ground Level (AGL) and the initial ballistic period of flight is ignored. The winds (selected from a sample RAWIN file) are again stored as a matrix in Winds(:,1:3) and approximated using piecewise cubic Hermite interpolating polynomials w(h), psi(h), and den(h).

```
%% Setting initial conditions
H = 7,000; g = 9.81; DR = 9;
h = linspace(0,H,100);
%% Producing spline interpolations for the winds and density
psih = pchip(Winds(:,1),Winds(:,2),h)*pi/180;
wh   = pchip(Winds(:,1),Winds(:,3),h);
den  = pchip(Winds(:,1),Winds(:,4),h);
```

Next, the rate of descent and gliding trajectory will be calculated based on the wind profile.

```
%% First Stage deployed
for i = 1:100
   DRv1(i) = DR * sqrt(den(1)/den(i));
end
```

```
Ind1 = 100;
for i = 1:Ind1-1
   xS1(i) = trapz(h(i:Ind1),wh(i:Ind1).*cos(psih(i:Ind1))./DRv1(i:Ind1));
   yS1(i) = trapz(h(i:Ind1),wh(i:Ind1).*sin(psih(i:Ind1))./DRv1(i:Ind1));
end
```

Now the total time to descend will be determined and the results plotted. This time calculation will be used in a new feature of the GUI that is explained in Section IV.

```
%% Calculate time to descend
t1 = trapz(h(1:Ind1),1./DRv1(1:Ind1));
```

The gliding trajectory of an unguided ADS using each algorithm is shown in Fig. 1 using a random wind sample from a RAWIN weather balloon. In this particular instance, the ballistic winds from 7,000 m AGL are 8.48 m/s. The star represents the release point.

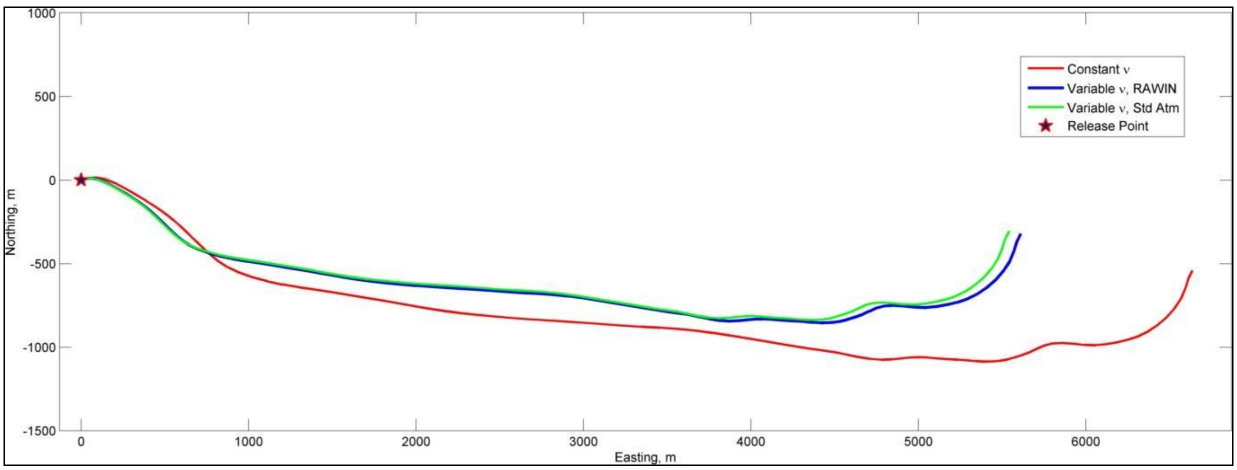

Figure 1. Gliding Trajectories.

The results of this example reveal that by incorporating a variable rate of descent (RAWIN), the total flight time decreases from 778 seconds (s) to 663 s, a difference of 115 s (14.8%). The difference in impact points is 1,048 m (15.6%). If the standard atmosphere calculations are used instead, the total flight time decreases from 778 s to 655 s, a difference of 123 s (15.8%), and the difference in impact points is 1,120 m (16.8%).

IV. Interactive GUI

Figure 2 shows the latest version of the GUI. As with the original version, this version of the GUI is subdivided into several panels which are described in detail below.

A. Starting the GUI

The GUI is started by running the GUIinitiation.m file in MATLAB. The user must manually choose a map file and time zone. The Drop Zone (DZ) list and Test System file are automatically selected. Descriptions of these file types are listed below.

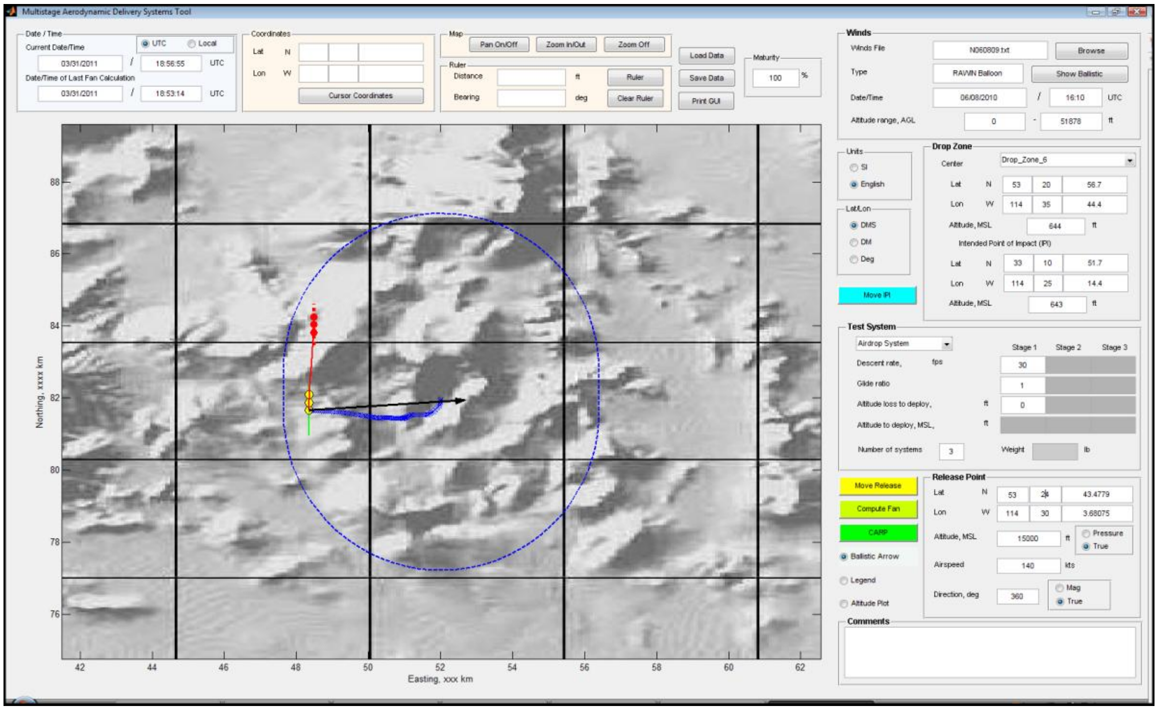

Figure 2. The 2nd Generation GUI.

Any map file in the jpeg format with rectangular UTM coordinates may be used in the GUI. In order for the GUI to read the jpeg map file, a same-name txt file describing the range of the coordinates must be created. For example, if using a map file labeled DZ_100k_UTM_WGS84.jpg, a txt file should be created and labeled DZ_100k_UTM_WGS84.txt. This txt file would contain the following:

UTMx range	23.65	57.93
UTMy range	30.17	116.51

The DZ List contains the DZs and their respective coordinates. This list will be made available in the GUI. The coordinates are geodetic coordinates with elevation listed in meters, MSL. An example is shown below:

DZ1	35 14 38.225075	134 26 39.21272	640.8660
DZ2	35 26 58.06226	134 26 26.53823	167.3258

The Test System File is an Excel spreadsheet that contains the various systems and their respective parameters. To add a new system simply add a row and fill in the empty cells. To delete a system simply delete the row containing that system. The GUI must be restarted for any changes to take effect.

A Time Zone Dialog allows the user to select one of five time zones for use in the GUI.

B. Interpreting the Outputs

The Map Display (Fig.3) is the graphical output of the GUI. Two layers are created in this display: the map and the SDZ. The map is loaded when the GUI is first started and can only be changed by restarting the GUI. The SDZ is created and altered when changes are introduced to the GUI by the user.

Although the inputs and outputs of the GUI are entered in a geodetic coordinate system, the map itself is graphically displayed using a UTM coordinate system. To reduce clutter on the display, the Y-Axis and X-Axis each display only two digits. Replacing the 'xx' with the correct two digit number and adding three zeros to the end will yield the actual UTM coordinates.

The IPI and release point are placed using the coordinates from the DZ panel and Release Point panel, respectively. The 20s Aircraft Track displays the flight path of the aircraft ±10 seconds from the release point. The ballistic trajectory is the expected path the test system will travel should the parachutes fail to open and the system fall ballistically to the ground. The gliding trajectory is the expected path of travel for an unguided test system. The fan represents the maximum possible area that the test system could travel within, incorporating both the test system parameters and wind profile. The symbols used to create the fan are listed in the legend panel.

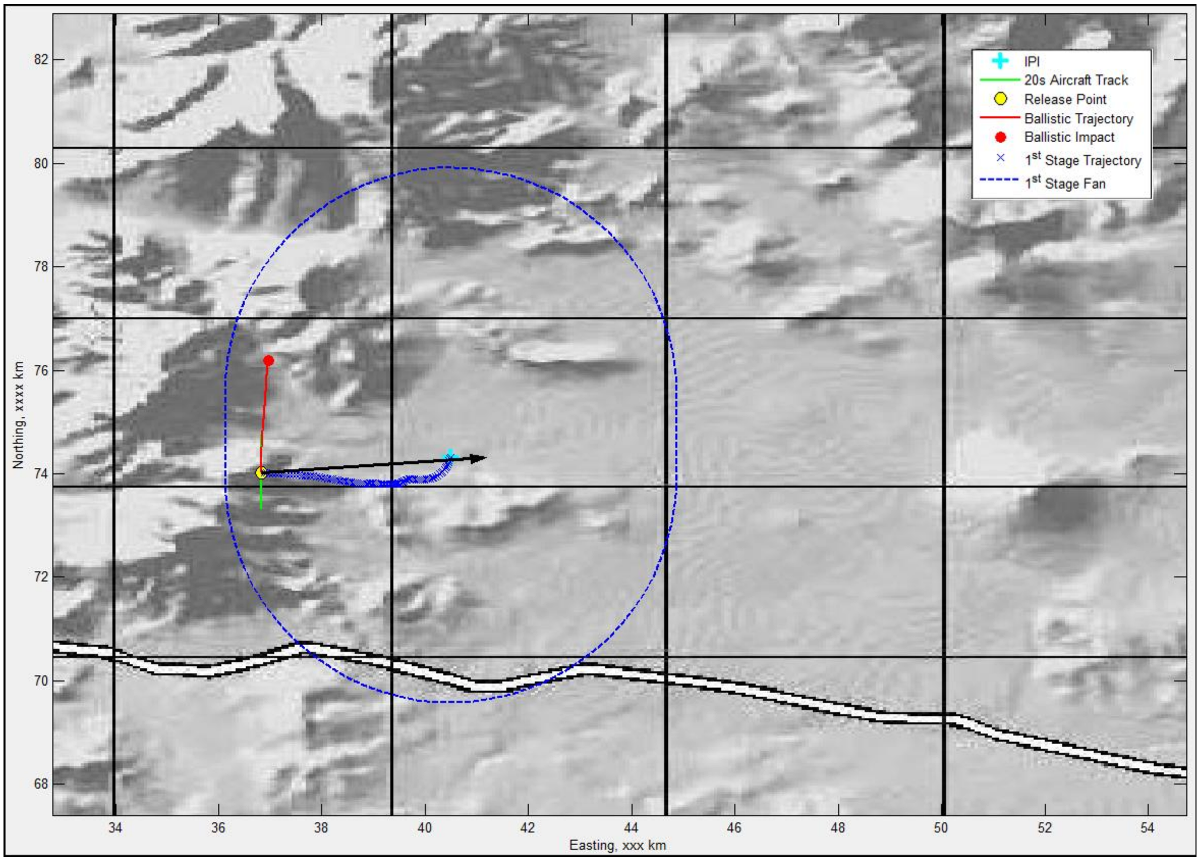

Figure 3. GUI Output.

A new feature in this GUI is the ability to incorporate topography into the SDZ calculation. If the maximum potential altitude of a system at any point within the safety fan is lower than the elevation at that point, the output will remove that point from the SDZ. This feature is still under development, but an example of this output is shown below in Fig.4. It can be seen that the SDZ has been reshaped to account for the higher elevation of the surrounding terrain.

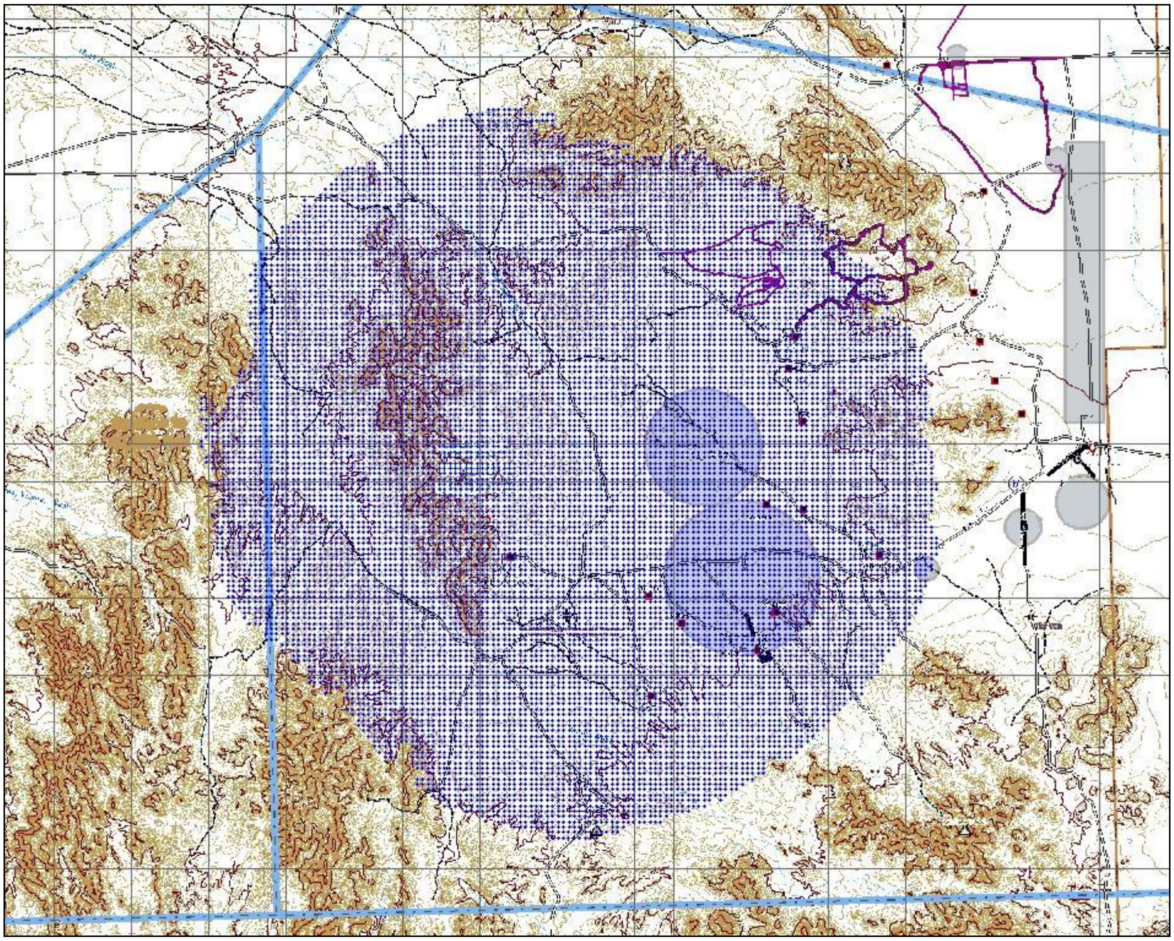

Figure 4. SDZ Incorporating Topography.

The Winds panel (Fig.5) allows the user to browse for and select wind files. The acceptable wind source files are sounding, Windpack, RAWIN balloon, and JAAWIN forecast. The "Show Ballistic" button computes the ballistic winds and graphically displays them to the user (Fig.6).

The Units panel (Fig.7) allows the user to choose between SI and English units in the GUI. The Lat/Lon panel allows the user to choose between various coordinate formats, including DMS (degree-minute-second), DM (degree-decimal minute), and Deg (decimal degree).

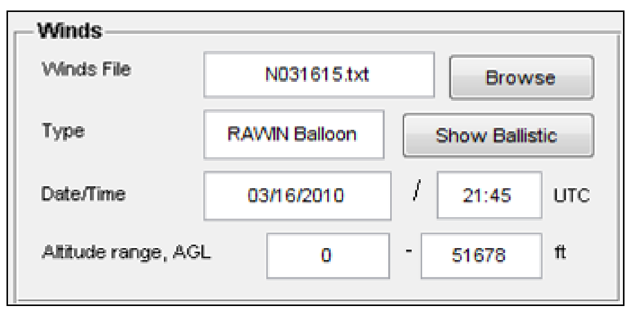

Figure 5. Winds Panel.

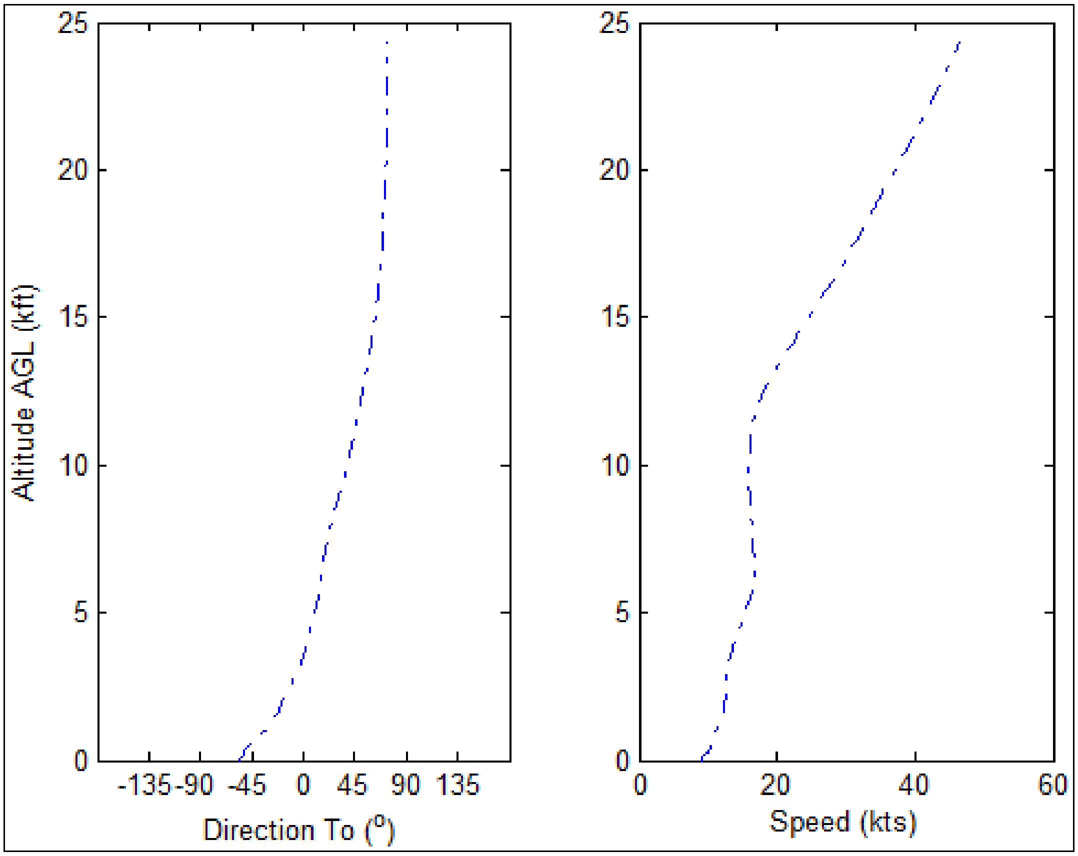

Figure 6. Ballistic Winds Profile.

The DZ panel (Fig.8) allows the user to select a DZ. Once a DZ is chosen, the remaining fields in the panel are automatically populated using the information contained in the DZ list file that was selected when the GUI was initialized. The map is then centered over the center of the DZ. The GUI initally assumes the IPI coordinates are the same as the DZ center coordinates; however, these coordinates may be changed using the Move IPI button.

Figure 7. Units Panel & Lat/Lon Panel.

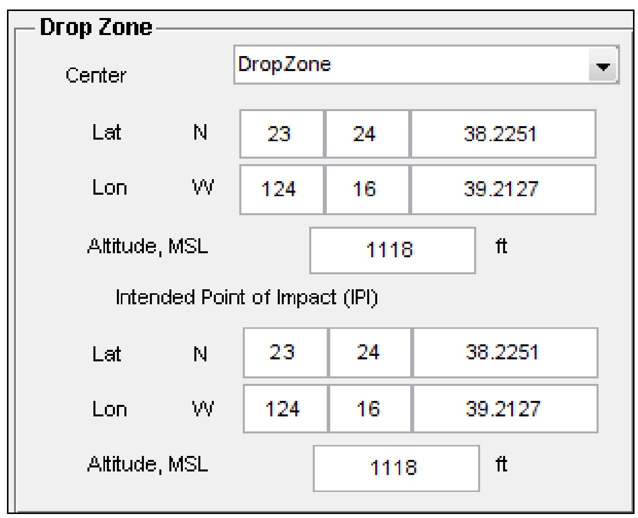

Figure 8. Drop Zone Panel.

The "Move IPI" button allows the user to enter new coordinates for the IPI. Upon pressing the button, the user is presented with an option of manually entering coordinates or clicking a point on the map (Fig.9). If the user selects to manually enter the coordinates, a new panel appears (Fig.10).

The Test System panel (Fig.11) allows the user to select an ADS from a drop down menu. The systems have been loaded directly from the Test System File. Once a system is chosen, the descent rate, glide ratio, altitude loss to deploy, and altitude to deploy are automatically populated in the blank fields. If a system has not been saved to the test system excel file, the user may choose "Create New" at the bottom of the list and manually enter the parameters.

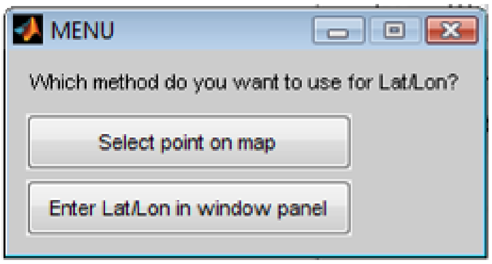

Figure 9. Move IPI Menu.

Figure 10. Move IPI Panel.

The third row of the Test System panel is labeled "Altitude loss to deploy". This is the altitude loss between aircraft exit and parachute deployment. The fourth row of the Test System panel is labeled "Altitude to deploy, MSL." This is the altitude at which the parachute deploys. A value may be entered in either the third or fourth row for each stage, but not both. It is assumed that the test system falls ballistically prior to deployment of the first stage parachute.

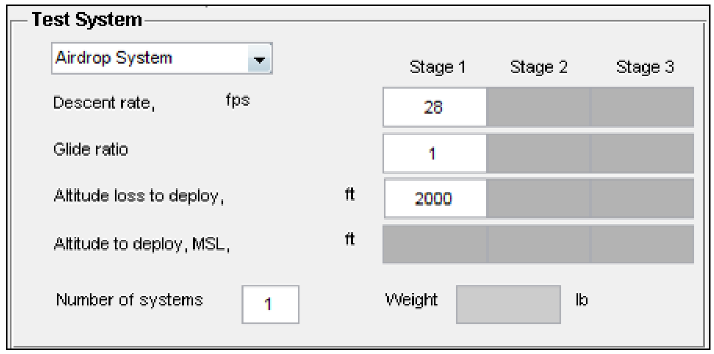

Figure 11. Test System Panel.

If multiple systems will be airdropped on a single pass, the user may enter the number of systems being airdropped and the GUI will automatically adjust the SDZ using a separation time of 3 seconds. The weight box is currently inactive but will become a user enabled box in a future version.

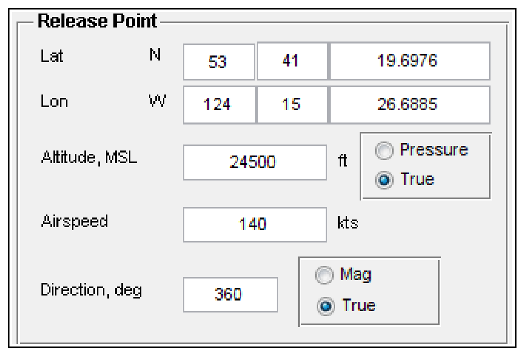

Figure 12. Release Point Panel.

The Release Point panel (Fig.12) allows the user to choose a release point, airdrop altitude, airspeed, and aircraft direction. The release point may be changed using the Move Release button described below. An option is given to enter direction in either degrees magnetic or degrees true. The magnetic declination used is 11 degrees, the current value at Yuma Proving Ground.

An option is also given to select either pressure altitude or true altitude. If pressure altitude is chosen, the GUI will use the international standard pressure datum of 1013.25 hPa and recalculate the true altitude by using either the RAWIN or JAAWIN data. Detailed calculations are presented in Section II.

The "Move Release" button allows the user to enter new coordinates for the release point. Upon pressing the button, the user is presented with an option of manually entering coordinates or clicking a point on the map (Fig.13).

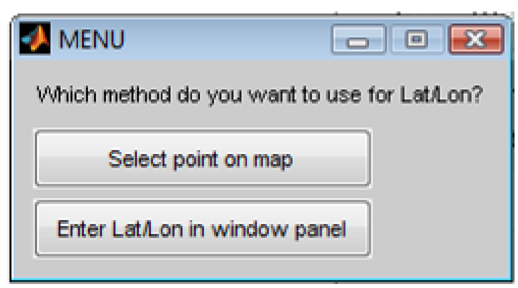

Figure 13. Move Release Menu.

If the user selects to manually enter the coordinates, a new panel appears (Fig.14).

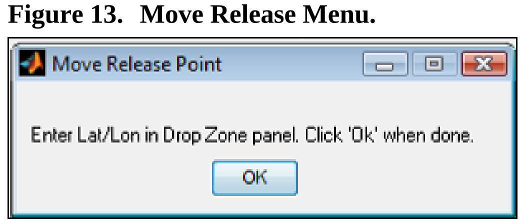

Figure 14. Move Release Point Panel.

The Compute Fan button is pressed to compute the SDZ using the data entered in the previously described panels. The SDZ is graphically overlaid on the imported map file. Details of the SDZ calculation are presented in Section II of this paper, as well as in Ref. 1.

The CARP button automatically adjusts the release point so that the final stage gliding trajectory ends at the IPI. If the elevation of the IPI does not match the elevation of the DZ, the GUI will adjust the release point so that the test system is over the IPI at the designated IPI altitude.

The Ballistic Winds Arrow button plots an arrow on the map, starting at the release point and pointing in the direction of the ballistic winds at the release altitude (Fig.15). This provides the user with a visual representation of the winds. The Legend button displays the various symbols used to graphically display the SDZ (Fig.16).

The Altitude Plot button plots a visual, two dimensional representation of the vertical flight of the test system (Fig.17). If pressure altitude was selected when computing the SDZ, the plot will display the true altitude and pressure altitude; otherwise, only the true altitude is displayed. The opening altitude of all stages is also displayed, relative to MSL. Between each stage, the altitude loss, descent time, and average descent velocity is shown. This plot helps to visually verify that all values were entered correctly into the GUI.

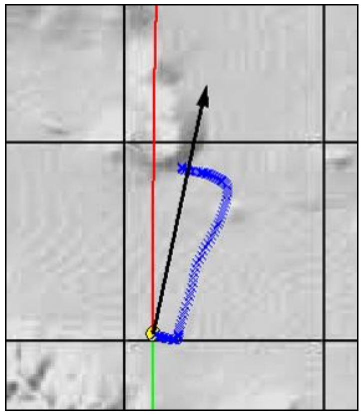

Figure 15. Ballistic Winds Arrow.

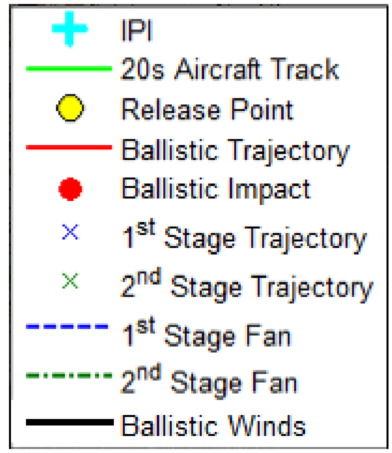

Figure 16. Legend Panel.

The Comments Box allows the user to attach notes to the GUI. Anything typed in the comments box is saved either through the use of the Save Data button or Print GUI button. The Date/Time panel (Fig.18) displays the current date and time, as well as the date and time of the last SDZ calculation. A radio button is also presented allowing the user to select between local time and UTC time. The Coordinates panel (Fig.19) allows the user to click a point on the map and see the coordinates for that point.

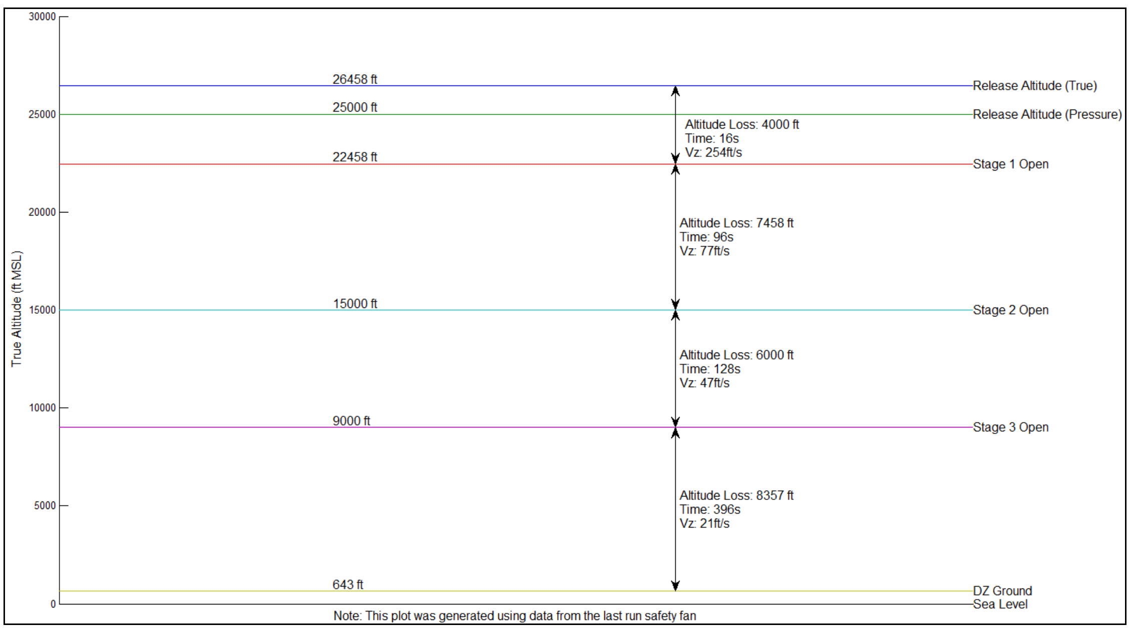

Figure 17. Altitude Plot.

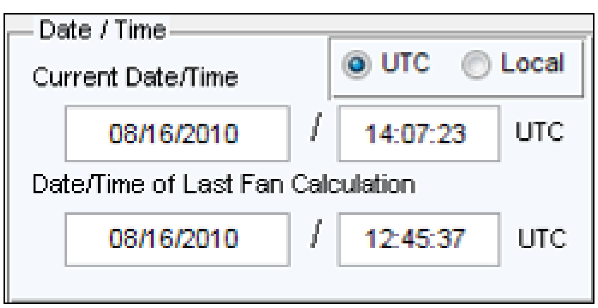

Figure 18. Date/Time Panel.

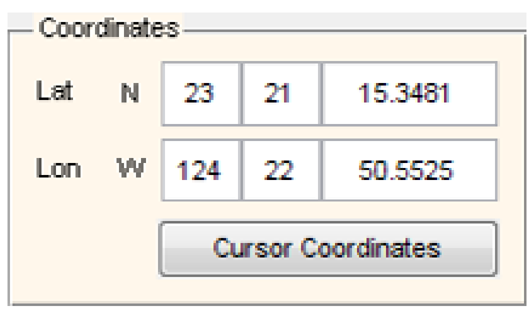

Figure 19. Coordinates Panel.

The Map panel (Fig. 20) allows the user to pan and zoom around the map. The Pan On/Off button creates a hand cursor so the map can be dragged/panned. The Zoom In/Off button creates a magnifying cursor so the map can be zoomed in and out. The Zoom Off button turns the zoom off and fits the entire map onto the screen.

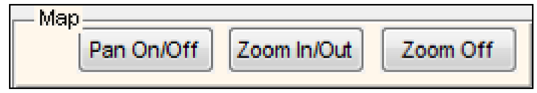

Figure 20. Map Panel.

The Ruler panel (Fig. 21) allows the user to find the distance and bearing between two points.

Figure 21. Rule Panel.

The GUI has the ability to save and load a data file containing previous GUI data. The Load Data button allows the user to load previously saved GUI data. The Save Data button allows the user to save the current GUI data for later use. The Print GUI button allows the user to save a screenshot of the GUI to a jpeg file.

The Maturity Box (Fig. 22) may be used when the confidence in the performance of a system is high enough to justify shrinking the size of the SDZ. This is normally done with high glide systems whose safety fans present logistical issues during testing. The value entered in this box should be determined after a thorough analysis of data. A value of 50%, for example, will reduce the SDZ to 50% of its original size. A value of 30% would reduce the fan to 30% of its original size.

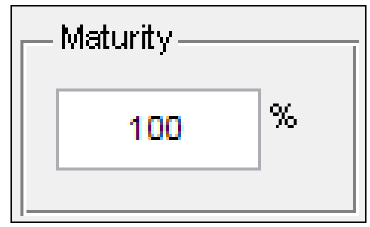

Figure 22. Maturity Box.

V. Future Developments

Future versions of the GUI will incorporate new features and further revisions to the formulas to increase the accuracy of the calculations. Some of the planned changes include:

a. Weight. The addition of a weight variable to the calculation will further increase the accuracy of calculations involving descent rate, and by extension, the gliding trajectory. For parafoil design parachutes there is no simple relationship between weight and rate of descent. Further analysis may yield a relationship that can then be incorporated in the GUI.

b. Fan Shape. A guided system with a large glide ratio poses many logistical issues due to the sheer size of its SDZ, especially when airdropped from high altitudes. An analysis of previous failures may shed light on the typical behavior of a failed system and help improve both the accuracy of the SDZ and the logistics of testing these systems.

c. Command Risk. Certain levels of risk in testing are considered acceptable if it can be proven that the level of risk for any given test meets the threshold specified by the Range Commanders Council. Using the results of the fan shape analysis above, future versions of the GUI can be coded to determine the probability of impacting a specified location within the SDZ.

VI. Conclusion

The developed tool has been used extensively by test planning officers in a field environment and the experience gained through this field use has contributed to the improvements and modifications of the tool. Revised algorithms have improved the accuracy of the computations, providing test officers with more reliable predictions on system behavior and ensuring the safety of those involved with testing. Additional features have increased ease of use and provide test officers with addition knowledge to assist with test planning. This paper detailed these improvements and modifications, presented the latest version of the tool, and discussed the planned future of the multistage aerodynamic delivery systems tool.

References

[1] Corley, M., and Yakimenko, O., "Computation of the Safety Fans for Multistage Aerodelivery Systems," *Proceedings of the 20th AIAA Aerodynamic Decelerator Systems Technology* Conference, Seattle, WA, May 4-7, 2009.

[2] *USAF Computed Air Release Point Procedures*, Air Force Manual 11-231, 31 August 2005.